A Spatially Constrained Temporally Adapted CBF Quantification Method for Arterial Spin Labeling (ASL) Perfusion MRI

Ze Wang[1]

[1]Departments of Psychiatry and Radiology, Perelman School of Medicine, University of Pennsylvania, Philadelphia, Pennsylvania, United States

Target audience: users of ASL MRI, and signal processing engineers.

Introduction. Advanced ASL CBF quantification (ASLq) is highly demanded due to the low signal-to-noise ratio (SNR) of ASL MRI [1]. This study was to evaluate a novel spatially constrained and temporally adapted (SCTA) ASLq method by exploiting two key aspects of ASL MRI: 1) adjacent voxels are highly correlated because of the systematic arterial spin labeling and because of that voxels from the same functional region are likely to have similar CBF; 2) ASL signal is modulated into the baseline MR signal which should be considered in ASLq.

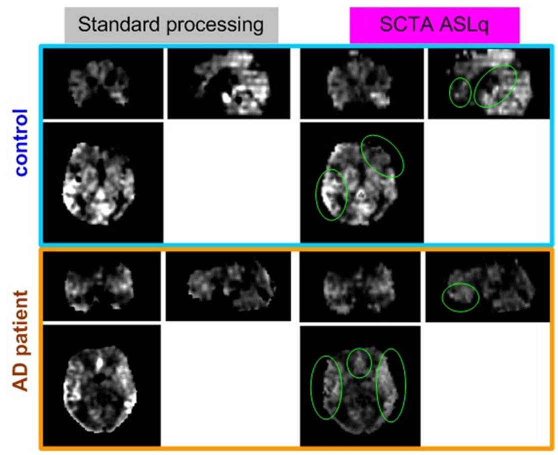

Fig. 1 CBF maps from two representative subjects.

Materials and Methods. Standard ASLq is equivalent to fitting the ASL MRI time series y to the boxcar spin labeling function x so that $\hat{y} = x\beta$ (β is the fitting coefficient representing ASL perfusion signal, $\hat{y}$ is an approximation to y) [3-5]. Suppose the control images are (c1, c2, c3, …). SCTA recreates x as x=(α*c1, c1, α*c2, c2, α*c3, c3, …)^T (α is a constant such as 95% after taking off the 5% change due to labeling), which is further constrained to be from the mean of the neighboring voxels to consider the spatial correlations. In this study, a regularized least square algorithm [9] was used to solve β, which was also constrained to be within a certain range around the mean β of the neighboring voxels. β was then converted into CBF using standard quantification model. The initial β value was obtained by fitting the global signal to the ideal spin labeling profile. To evaluate SCTA, repeat ASL data were acquired from 16 Alzheimer's Disease (AD) patients and 20 age matched controls with IRB approval and signed written consents. Data acquisition details were given in previous study [7]. ASL images were preprocessed using ASLtbx with state-of-art denoising procedures [3-5]. In SCTA, 4 surrounding voxels were used. The constraint range for β was set to be from 0 to 2 times of the mean coefficient of the neighboring voxels. SPM was used to map each individual brain into the MNI space. Region-of-interests (ROIs) were defined in grey matter (GM) and white matter (WM). SNR was calculated as the ratio of the mean GM CBF/std of the WM CBF. The intraclass correlation coefficient (ICC) between the two scan's global CBF was calculated. A two sample t-test was performed to assess the control versus patient CBF difference.

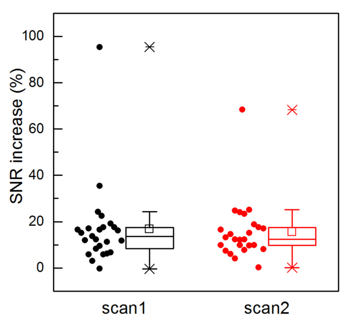

Fig. 2. SNR increase of SCTA ASLq.

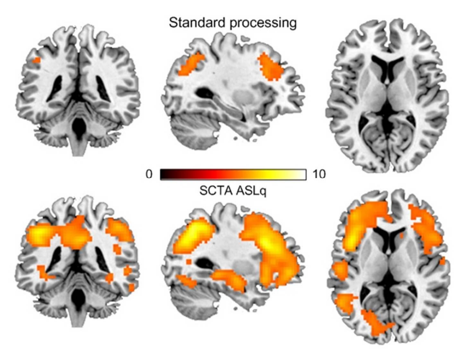

Fig. 3. Hypoperfusion patterns in AD patients identified at p<0.05 (FWE corrected).

Results and Discussion.

In Fig 1, as compared to the current ASLq, SCTA ASLq remarkably improved CBF quality in several brain regions as marked by the green ovals, including signal recovery in right prefrontal and medial orbito-frontal (mOFC) cortex suppressing the superficial "high" CBF in the subarachnoid space in insula, mOFC, and superior temporal cortex. Using the controls' data, Fig.2 shows that SCTA ASLq provided >15% SNR increase as compared to the state-of-arts for both scan sessions (p<1e-4). Using SCTA ASLq, we observed a 2.12% ICC increase for the whole brain CBF. Fig. 3 shows that SCTA ASLq magnificently improved the sensitivity of ASL MRI for detecting the well-confirmed hypoperfusion patterns in parietal cortex, precuneus, prefrontal and temporal cortex in AD patients [7-8].

In conclusion, we proposed and verified a novel signal processing method for ASLq, which increased SNR, ICC, and sensitivity of ASL perfusion MRI for a clinical application.

Acknowledgement This work was supported by NIH grants: R21DC011074 and RR02305, and the UPenn-Pfizer Alliance fund.

Reference [1] Detre, JMRI, 2012, 1026-37. [2] Wang et al, MRI, 26, 261-269, 2008. [3] Behzadi et al, Neuroimage, 2007, 90-101. [4] Hernandez-Garcia et al, MRI 2010, 919-27, [5] Wang MRI, 2012, 1409-15. [6] Hansen PC *Rank-Deficient and Discrete Ill-Posed Problems:Numerical Aspect of Linear Inversion, 1998.* [7] Zhang et al, JAD, 2012, 677-87. [8] Alsop et al, Neurology 2000.